ANNALS of Clinical and Translational Neurology
Open Access
ANA American Neurological Association since 1875

RESEARCH ARTICLE

Diagnostic utility of ASL-MRI and FDG-PET in the behavioral variant of FTD and AD

Duygu Tosun[1], Norbert Schuff[1], Gil D. Rabinovici[2], Nagehan Ayakta[2,3], Bruce L. Miller[2], William Jagust[3], Joel Kramer[2], Michael M. Weiner[1] & Howard J. Rosen[2]

[1]Department of Radiology and Biomedical Imaging, University of California, San Francisco, California
[2]Memory and Aging Center, Department of Neurology, University of California, San Francisco, California
[3]School of Public Health, University of California, Berkeley, California

Correspondence
Duygu Tosun, Assistant Professor in Radiology and Biomedical Imaging, University of California, San Francisco (UCSF), Center for Imaging of Neurodegenerative Diseases (CIND) VA Medical Center, 4150 Clement St., Bldg 13, 114M, San Francisco, CA 94121. Tel: 415 221 4810 ext 3650; Fax: (415) 386-3954; E-mail: duygu.tosun@ucsf.edu

Funding Information
This work was supported by the National Institutes of Health Grant P01 AG019724-11, K24 AG045333, R01 AG032306, R01-AG038791, and P50 AG023501, The Hillblom Network, and the Department of Defense Grant W81XWH-05-2-0094. This work has also been made possible by use of research facilities at the Veteran Affairs Medical Center in San Francisco.

Received: 3 May 2016; Revised: 6 June 2016; Accepted: 8 June 2016

Annals of Clinical and Translational Neurology **2016; 3(10): 740–751**

doi: 10.1002/acn3.330

Abstract

Objective: To compare the values of arterial spin-labeled (ASL) MRI and fluorodeoxyglucose (FDG) PET in the diagnosis of behavioral variant of frontotemporal dementia (bvFTD) and Alzheimer's disease (AD). **Methods**: Partial least squares logistic regression was used to identify voxels with diagnostic value in cerebral blood flow (CBF) and cerebral metabolic rate of glucose (CMRgl) maps from patients with bvFTD ($n = 32$) and AD ($n = 28$), who were compared with each other and with cognitively normal controls (CN, $n = 15$). Diagnostic values of these maps were compared with each other. **Results**: Regions that differentiated each disorder from controls were similar for CBF and CMRgl. For differentiating AD from CN, the areas under the curve (AUC) for CBF (0.89) and CMRgl (0.91) were similar, with similar sensitivity (CBF: 86%, CMRgl: 78%) and specificity (CBF: 92%, CMRgl: 100%). Likewise, for differentiating bvFTD from CN performances of CBF (AUC = 0.83) and CMRgl (AUC = 0.85) were equivalent, with similar sensitivity (CBF: 78%, CMRgl: 79%) and specificity (CBF: 92%, CMRgl: 100%). In differentiating bvFTD from AD, classification was again similar for CBF (AUC = 0.87) and CMRgl (AUC = 0.79), as were sensitivity (CBF: 83%, CMRgl: 89%) and specificity (CBF: 93%, CMRgl: 78%). None of the differences in any performance measure were statistically significant. **Interpretation**: ASL-MRI has similar diagnostic utility as FDG-PET in the diagnosis of AD and bvFTD. Continued development of ASL-MRI as a diagnostic tool for neurodegenerative dementias is warranted.

Introduction

Frontotemporal lobar degeneration (FTLD) is the second most common form of neurodegenerative dementia in the presenile population and the third most prevalent form of neurodegenerative dementia overall.[1,2] With an estimated prevalence of 15/100,000 in the age group of 45–64 years, FTLD represents a significant challenge for social welfare.[1,3] FTLD can present with a variety of syndromes, including progressive supranuclear palsy, corticobasal degeneration, and progressive aphasia, but the most common presentation is progressive change in personality with abnormalities in socioemotional behavior, referred to as the behavioral variant of frontotemporal dementia (bvFTD).[4] Diagnosis of bvFTD remains difficult, with patients being erroneously diagnosed with Alzheimer's disease (AD) or psychiatric disorders.[5–7] A large body of work has demonstrated that brain imaging, in particular structural magnetic resonance imaging (MRI) and functional imaging of cerebral blood flow (CBF) with SPECT or cerebral metabolic rate of glucose (CMRgl) with fluorodeoxyglucose (FDG) positron emission tomography (PET), can improve the accuracy of differential diagnosis in bvFTD.[8–17] These findings led the Center for Medicare and Medicaid Services (CMS) to approve FDG-PET as a diagnostic test for differentiating bvFTD

from AD (https://www.cms.gov/medicare-coverage-database/details/ncd-details.aspx?NCDId=288&ncdver=3&bc=BAABAAAAAAAA&).

Recent studies have indicated that measurement of CBF using arterial spin labeling (ASL) MRI is also abnormal in neurodegenerative disease, and can improve differential diagnosis of bvFTD.[18–20] BvFTD shows frontal patterns of hypoperfusion, even after controlling for loss of brain volume, as compared with AD, which is associated with relative hypoperfusion in the parietal regions. These patterns are similar to those observed with SPECT perfusion and FDG-PET.[21–24] One study has demonstrated that ASL-MRI improves diagnostic classification of bvFTD versus age-matched controls.[19] In AD, studies have demonstrated that patterns of CBF deficits detected with ASL-MRI are roughly similar to metabolic deficits identified using FDG-PET,[25–27] and that both imaging modalities have similar diagnostic value in AD.[26] Although recent studies have indicated that patterns of CBF abnormalities and patterns of metabolic deficits are also similar in bvFTD,[25] no studies have yet compared the diagnostic value of CBF measures from ASL-MRI with the diagnostic utility of CMRgl measures from FDG-PET in differentiating bvFTD from other dementias such as AD. If ASL-MRI could be demonstrated to have similar utility as FDG-PET for diagnosis and quantification of regional functional deficits in bvFTD this could be very beneficial for research studies that might use functional imaging to track disease, and for clinical assessments because ASL-MRI can be obtained more conveniently than FDG-PET, with less expense and no exposure to radiation. Therefore, the goal of the current study was to compare the diagnostic value of these two neuroimaging techniques in differentiating bvFTD from AD.

Methods

Participants

The study included 32 patients with bvFTD, 28 patients with AD, and 15 clinically normal (CN) elderly individuals. The study sample was selected from the University of California – San Francisco (UCSF) Memory and Aging Center database based on the availability of ASL-MRI as well as FDG-PET scans. Both neuroimaging evaluations occurred within a 180-day period. Participants were consecutively recruited from large studies of FTLD and related disorders (P01-AG019724, P50-AG023501, R01-AG032306, R01-AG038791). Patients were diagnosed using published criteria[28,29] after a comprehensive evaluation at the UCSF Memory and Aging Center including neurological history and examination, nursing assessment, laboratory evaluation, and a previously described neuropsychological assessment of memory, executive function, language, and mood.[30] The majority of bvFTD patients were diagnosed using the consensus criteria published in 1998, which include imaging as a potentially supportive feature but do not require imaging findings for diagnosis. Because of our interest in examining the value of imaging in diagnosis, our center has never used imaging to arrive at a consensus diagnosis in our research programs. New criteria for bvFTD were published in 2011.[31] These guidelines simplify the clinical criteria and more formally incorporate brain imaging in the diagnosis of bvFTD, requiring imaging findings for a "probable" diagnosis. In moving to this diagnostic system our center continued to determine diagnosis before examining imaging data, so that cases diagnosed with bvFTD using this system would meet criteria for possible but not necessarily probable bvFTD. The neuropsychological assessment battery includes the mini-mental state examination (MMSE),[32] tests of working memory (digit span backwards), visuospatial function (copy of a complex figure), visuospatial memory (memory of a figure after 10 min), confrontational naming (15 items from the Boston Naming Test[33]), a brief syntax comprehension task with five questions requiring participants to point to pictures corresponding to specific sentences (e.g., point to the picture of the woman being kissed by the man), five calculations, set-shifting (modified version of the Trails B task[34]), and tests of verbal fluency (words beginning with the letter "D" or "H" and animals) and nonverbal fluency (design fluency[35]). The Geriatric Depression Scale (GDS[36]) is used to assess mood. Level of functional impairment was quantified using the Clinical Dementia Rating Scale (CDR).[37] Patients with an AD diagnosis but who were amyloid negative based on in vivo imaging or cerebrospinal fluid sampling were excluded.

CN individuals were required to have no cognitive complaints, no cognitive or behavioral difficulties identified by a knowledgeable informant, and they underwent the same neuropsychological testing as patients. Because normal variation in cognitive performance encompasses a wide range of scores, no specific cognitive cutoffs were used for inclusion in the control group. Neuroimaging protocols for the CN individuals were same as the ones used for bvFTD and AD patients.

The study was approved by the UCSF and Lawrence Berkeley National Laboratory committees on human research, and all subjects provided written, IRB-approved informed consent before participating.

MRI acquisition

All MRIs were acquired on a 3.0 Tesla Siemens (Siemens, Iselin, NJ) TIM Trio scanner equipped with a 12-channel head coil located at the UCSF Neuroscience Imaging

Center. Whole brain structural MR images were acquired using volumetric magnetization prepared rapid gradient-echo sequence (MPRAGE; TR/TE/TI = 2300/2.98/900 msec, $\alpha = 9°$). The field of view was 240 × 256 mm, with 1 × 1 mm in-plane resolution and 1 mm slice thickness. Perfusion images were acquired using a pulsed arterial spin labeling (ASL) sequence[38] with a single-shot echo-planar imaging (EPI) part to map the perfusion signal. ASL-MRI was performed with TR/TE = 2500/11 msec and a postlabeling delay of 1800 msec to allow the arterial spin labels perfuse completely into brain tissue. Sixteen slices, each 6-mm thick with a 7.2-mm center to center distance and 4 × 4 mm^2 in-plane resolution were acquired.

PET acquisition

All subjects underwent PET imaging with [^{18}F] FDG at Lawrence Berkeley National Laboratory on a Siemens ECAT EXACT HR or on a Siemens Biograph Truepoint 6 scanner in three-dimensional acquisition mode. Tracer synthesis, PET acquisition, and preprocessing were performed as previously described.[39] Thirty minutes of dynamic FDG data (t = 30–60 min postinjection) were obtained. Ten-minute transmission scans for attenuation correction or X-ray CT were obtained either immediately before or after each [^{18}F] FDG scan. PET data were reconstructed using an ordered subset expectation maximization algorithm with weighted attenuation. Images were smoothed with a 4-mm Gaussian kernel with scatter correction. All images were evaluated before analysis for patient motion and adequacy of statistical counts.

Image processing

Quantitative maps of CBF were obtained from the ASL-MRIs following a largely automated pipeline, including motion correction, nonlinear geometric distortion correction, dynamic data fitting to a dual compartment perfusion model, which takes into account variable transit times, bolus durations, distributed concentrations of capillary water and restricted brain–blood barrier permeability, and intensity normalization to average CBF measurement from primary motor cortex.[40]

Maps of cerebral metabolic rate for glucose (CMRgl) were obtained from FDG-PET images preprocessed at the University of California – Berkeley, following a standardized procedure described previously.[41] Briefly, FDG-PET frames were summed and standard uptake volume ratios (SUVR) were calculated by normalizing the summed FDG image to mean activity in the pons for each subject.[42]

First imaging frames of ASL-MRI and FDG-PET data were coregistered to the subject's structural MRI using boundary-based registration.[43] The derived coregistration parameters were applied to the subject's CBF and CMRgl images. To allow across-subject comparisons, each subject's structural MRI was diffeomorphically mapped to an unbiased structural MR image template using advanced normalization tools (ANTs).[44] The derived normalization parameters were applied to the subject's coregistered CBF and CMRgl images. Normalized CBF images were smoothed with a Gaussian kernel of 8 mm full-width half-max to match intrinsic smoothness of CMRgl maps. In this study, neither CBF nor CMRgl images were corrected for partial volume effects.

Statistical analysis

A general linear model-based detrending method was used to control for normal confounding effects of age, sex, and education, based on the 15 CN subjects. In addition, CMRgl maps were further corrected for potential confounding effects due to scanner differences. Adjusted maps of CBF and CMRgl were used for further data analyses.

To generate maps of regional CBF and CMRgl abnormalities relative to CN subjects for each diagnostic group (bvFTD or AD) separately, we conducted a modality-specific partial least squares (PLS) logistic regression model with the imaging measures from each gray matter tissue voxel in the template image space as predictors and the diagnosis (bvFTD vs. CN or AD vs. CN) as a dichotomized outcome. The analysis was repeated with bvFTD versus AD as the dichotomized outcome to generate maps of imaging abnormalities that best discriminate bvFTD and AD subjects.

The motivation for use of PLS logistic regression model over voxel-wise logistic regression model is as follows: high-dimensional data, such as voxel-based MR and PET images, based on a relatively small number of participants inherently comes with significant codependencies and contain a large number of association patterns, most of which are erroneous or redundant. Our goal was to identify which of these are significant associations, with high classification power. PLS regression[45] has the ability to handle high-dimension, low sample size, multicollinear data, while searching for modes that explain the maximum covariance between the explanatory and response spaces. The PLS regression is a supervised dimensionality reduction technique based on a latent decomposition model. Furthermore, unlike commonly used multivariate latent decomposition approaches such as principal component regression or canonical correlation analysis,[46] where the dimensionality reduction of the data is carried out independent of the response variable by maximizing the variance within the

regressors alone, PLS models the regression by maximizing the covariance between the regressors and response. The latent components are extracted in the regressor and response data spaces such that the covariance between the two is maximized. The statistical significances of the CBF and CMRgl latent variables inferred by these PLS logistic regression models were assessed using the projected data and nonparametric permutation testing. All statistical computations were carried out using the statistical package R.

To assess whether the PLS method generated maps that were different than maps that would be generated using more traditional methods of group comparison for brain imaging, CBF and CMRgl maps were also analyzed on a voxel-by-voxel basis using nested general linear models (GLMs) constructed with and without the group effect term (bvFTD vs. CN or AD vs. CN or bvFTD vs. AD) and compared using maximum likelihood ratio (MLratio) tests. Age, gender, and education were included as covariates. GLMs for CMRgl maps further included scanner model as a potential confounding factor. The resulting statistical parametric maps were thresholded to control for multiple comparisons using the false discovery rate (FDR) with $q = 0.05$.

Discriminative power of CBF and CMRgl changes

PLS regression is a supervised dimensionality reduction technique to extract a small number of latent components or projection scores that are linear combinations of the original variables to avoid multicollinearity. Using this property of PLS regression, neuroimaging-based scores for each diagnostic group were calculated by projecting each individual's neuroimaging data onto the latent variable inferred by the corresponding PLS logistic regression model. This was done for CBF and CMRgl measures separately.

Logistic regression-based classification models were used to assess the discriminative power of CBF-based and CMRgl-based scores in differentiating (1) bvFTD subjects from CN subjects; (2) AD subjects from CN subjects; and (3) bvFTD subjects from AD subjects. Performance of these classification models was estimated in a leave-one-out (LOO) framework with area under the curve (AUC), sensitivity (SENS), and specificity (SPEC) metrics. At each LOO iteration, PLS-based dimensionality reduction was repeated with the entire cohort minus the subject left out for model validation. Sensitivity and specificity were estimated by the appropriate observed proportion and 95% CI were generated based on the assumption that they follow a binomial distribution. Sensitivity and specificity of CBF-based and CMRgl-based scores were compared using McNemar test.[47]

Results

Demographic characteristics

Demographic characteristics of the subjects are summarized in Table 1. On average bvFTD subjects were significantly younger than CN subjects ($t = 2.13$; $P = 0.04$), but not than AD subjects ($t = 1.47$; $P = 0.15$). Both bvFTD and AD subjects performed significantly worse than CN subjects on MMSE ($t = 5.44$; $P = 3.09\text{e-}06$ and $t = 8.16$; $P = 4.58\text{e-}09$, respectively). Furthermore, AD subjects performed significantly worse than bvFTD subjects on the MMSE ($t = 4.75$; $P = 2.53\text{e-}04$). Both bvFTD and AD subjects had significantly higher CDR than CN subjects ($t = -9.84$; $P = 6.32\text{e-}12$ and $t = -9.30$; $P = 4.42\text{e-}11$, respectively). In addition, bvFTD subjects' CDR scores were significantly higher than those of AD subjects ($t = 2.08$; $P = 0.04$).

Voxel-wise CBF and CMRgl group differences

Raw unprocessed images from each diagnosis and modality are shown in Figure 1. As shown in Figure 2A–B, AD

Table 1. Demographic and clinical characteristics of study participants.

	CN	bvFTD	AD
N	15	32	28
Age (years)	65.8 ± 6.70	61.375 ± 6.51[1]	64.21 ± 8.17
Gender (F/M)	6/9	11/21	14/14
Education (years)	16.8 ± 2.48	16.10 ± 3.28	16.89 ± 3.22
Time between ASL-MRI and FDG-PET (days)	24.67 ± 19.29	20.22 ± 31.53	37.96 ± 37.96
MMSE	29.07 ± 1.22	24.74 ± 4.06[2]	17.11 ± 7.57[3]
CDR	0 ± 0	1.20 ± 0.63[4]	0.91 ± 0.45[5]

CDR, Clinical Dementia Rating Scale. CN, cognitively normal controls.
[1]Statistically different than CN (two-sample *t*-test; $t = 2.13$; $P = 0.04$).
[2]Statistically different than CN (two-sample *t*-test; $t = 5.44$; $P = 3.09\text{e-}06$).
[3]Statistically different than CN (two-sample *t*-test; $t = 8.16$; $P = 4.58\text{e-}09$) and than bvFTD (two-sample *t*-test; $t = 4.75$; $P = 2.53\text{e-}04$).
[4]Statistically different than CN (two-sample *t*-test; $t = -9.84$; $P = 6.32\text{e-}12$).
[5]Statistically different than CN (two-sample *t*-test; $t = -9.30$; $P = 4.42\text{e-}11$) and than bvFTD (two-sample *t*-test; $t = 2.08$; $P = 0.04$).

patients had predominantly frontoparietal and temporal hypoperfusion and bvFTD patients had predominantly frontotemporal hypoperfusion, both relative to CN subjects. In direct comparison of patient groups, bvFTD patients displayed frontotemporal hypoperfusion relative to AD patients, and AD patients had diffused hypoperfusion in parietal brain regions compared to bvFTD patients.

Whole brain patterns of CBF and CMRgl abnormalities best differentiating AD and bvFTD patients from controls

Figure 3 shows the spatial signatures of the whole brain patterns of CBF and CMRgl abnormalities in each diagnostic group (i.e., bvFTD and AD) relative to CN subjects as inferred by PLS logistic regression. Cold colors indicate hypoperfusion and hypometabolism detected by ASL-MRI and FDG-PET, respectively. Hot colors indicate hyperperfusion and hypermetabolism detected by ASL-MRI and FDG-PET, respectively. Dark hot/cold colors indicate greater contribution of the local CMRgl and CBF variations to the AD versus CN (Fig. 3A) and bvFTD versus CN (Fig. 3B) separation.

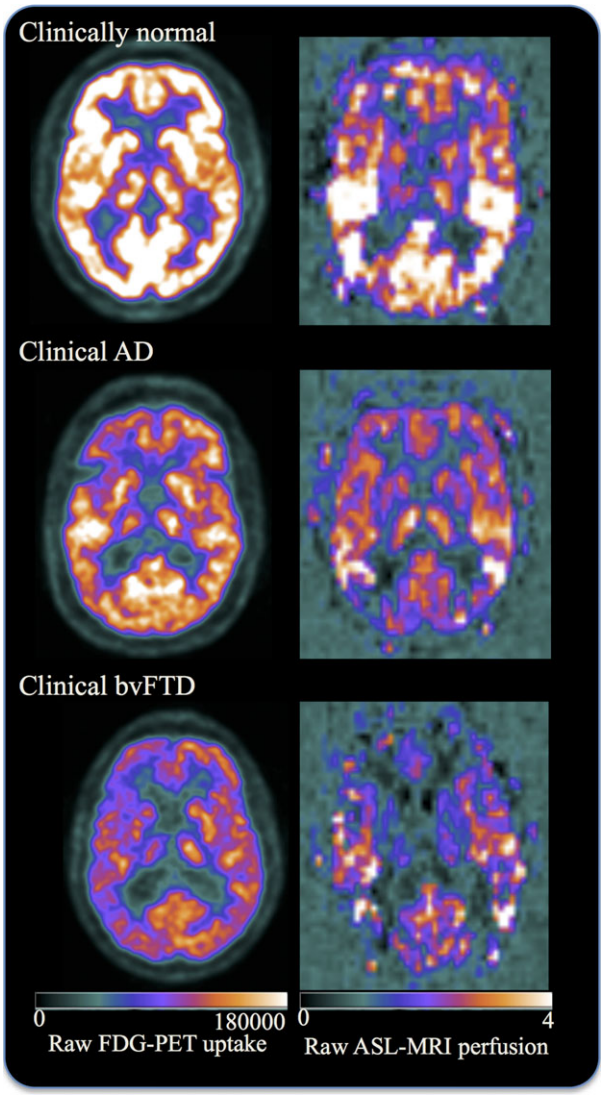

Figure 1. Raw FDG-PET uptake and raw ASL-MRI perfusion maps in selected participants. Images are displayed in neurologic orientation.

Overall, the spatial signatures of the two modalities were similar in each disorder. Relative to CN subjects, AD subjects had both hypoperfusion and hypometabolism in the parietotemporal brain regions including the precuneus, inferior parietal lobule, supramarginal, superior parietal, postcentral, fusiform, inferior temporal, middle temporal, and superior temporal gyri, as well as in the cingulate, inferior frontal, inferior occipital, and superior occipital gyri. In addition, AD patients had hypoperfusion but no significant CMRgl abnormality in the hippocampus, lingual gyrus, cuneus, and putamen regions.

In bvFTD, extensive regions of hypoperfusion and hypometabolism are seen in frontotemporal brain regions including medial and lateral fronto-orbital, inferior frontal, middle frontal, superior frontal, fusiform, inferior temporal, middle temporal, superior temporal gyri and gyrus rectus, cingulate, precuneus, and insular cortex. bvFTD patients exhibited hypoperfusion in hippocampus, cuneus, and lingual and inferior occipital gyri, and caudate nucleus without any significant CMRgl abnormalities.

Whole brain patterns of CBF and CMRgl abnormalities best differentiating AD and bvFTD patients

Figure 4 shows the spatial signatures of the whole brain patterns of relative CBF and CMRgl abnormalities as inferred by PLS logistic regression in direct differentiation of bvFTD and AD patients. Cold colors indicate hypoperfusion and hypometabolism in bvFTD relative to AD detected by ASL-MRI and FDG-PET, respectively. Hot colors indicate hyperperfusion and hypermetabolism in bvFTD relative to AD detected by ASL-MRI and FDG-PET, respectively. Dark hot/cold colors indicate greater contribution of the local CMRgl and CBF variations to the AD versus bvFTD separation. In direct bvFTD versus AD classification analysis, both CBF and CMRgl differences contributed to separation between the two groups in a similar spatial pattern of a diffuse set of cortical and subcortical regions, mostly in the parietal and frontal regions including precuneus, superior parietal, medial fronto-orbital gyrus, and gyrus rectus, along with cuneus, and superior occipital gyrus (Fig. 4). There were a few regions where only hypometabolism in AD relative

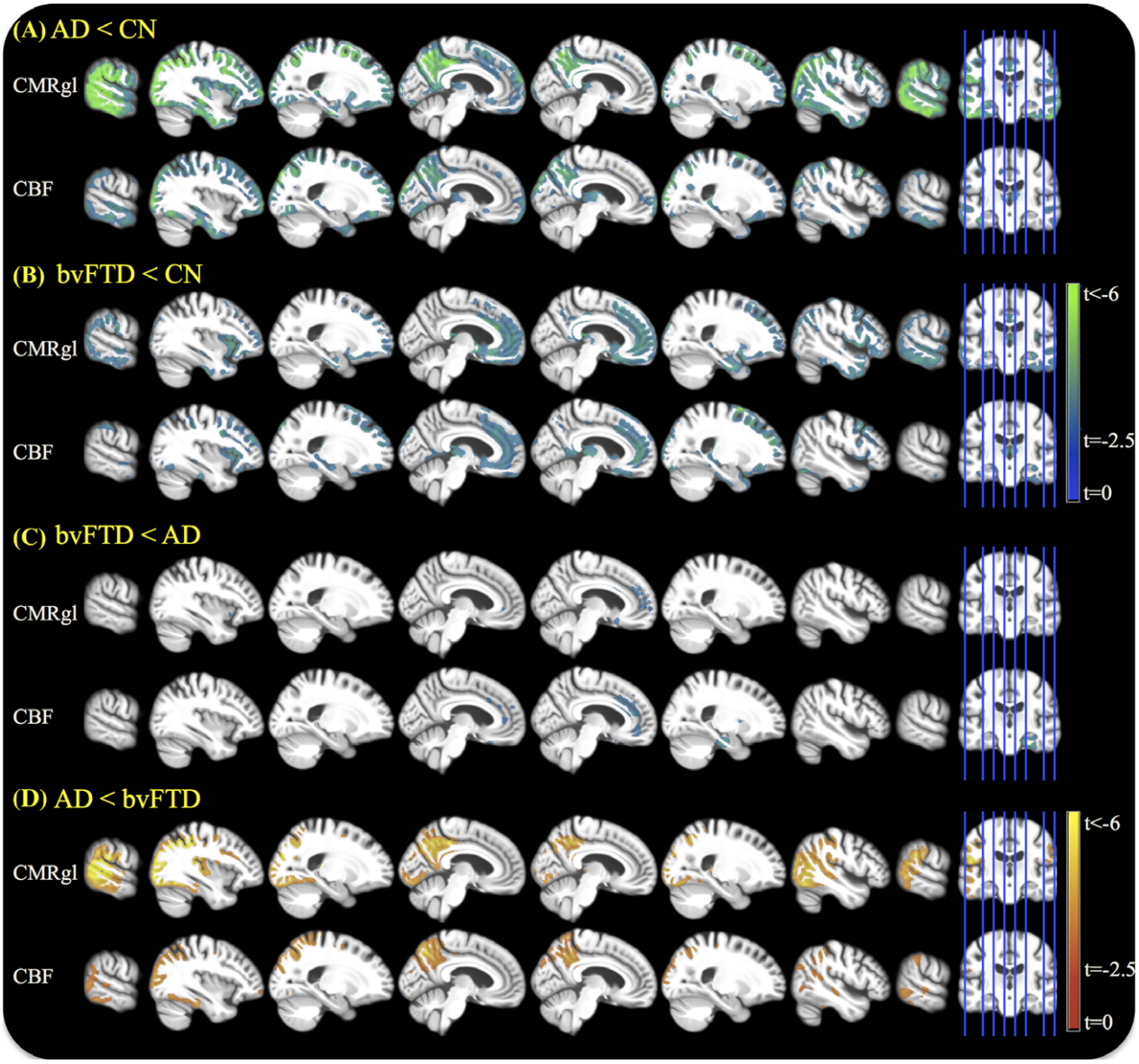

Figure 2. Voxel-wise group comparison based on generalized linear regression model with age, gender, education, and study stage as covariates. Images are displayed in neurologic orientation.

to bvFTD contributed to group separation including the middle frontal and lateral fronto-orbital gyrus. In contrast, only hypoperfusion in AD relative to bvFTD in inferior temporal, and only hypoperfusion in bvFTD relative to AD in insular cortex, cingulate gyri, and amygdala contributed to group separation.

Discriminative power of CBF and CMRgl changes

Receiver operating characteristic (ROC) curves in Figure 5 and details in Table 2 show the estimated performances of the logistic regression classifiers with CBF-based and CMRgl-based scores separately for each pairwise diagnostic group classification.

In AD versus CN classification, areas under the curve for CMRgl-based (0.91, 95% CI: 0.77–1.00) and CBF-based scores (0.89, 95% CI: 0.76–1.00) were similar with similar sensitivity (CMRgl-based 78%, CBF-based 86%) and specificity (CMRgl-based 100%, CBF-based 92%).

Similarly, performance of CMRgl-based (AUC = 0.85, 95% CI: 0.70–0.99) and CBF-based scores (AUC = 0.83, 95% CI: 0.68–0.98) were similar in bvFTD versus CN

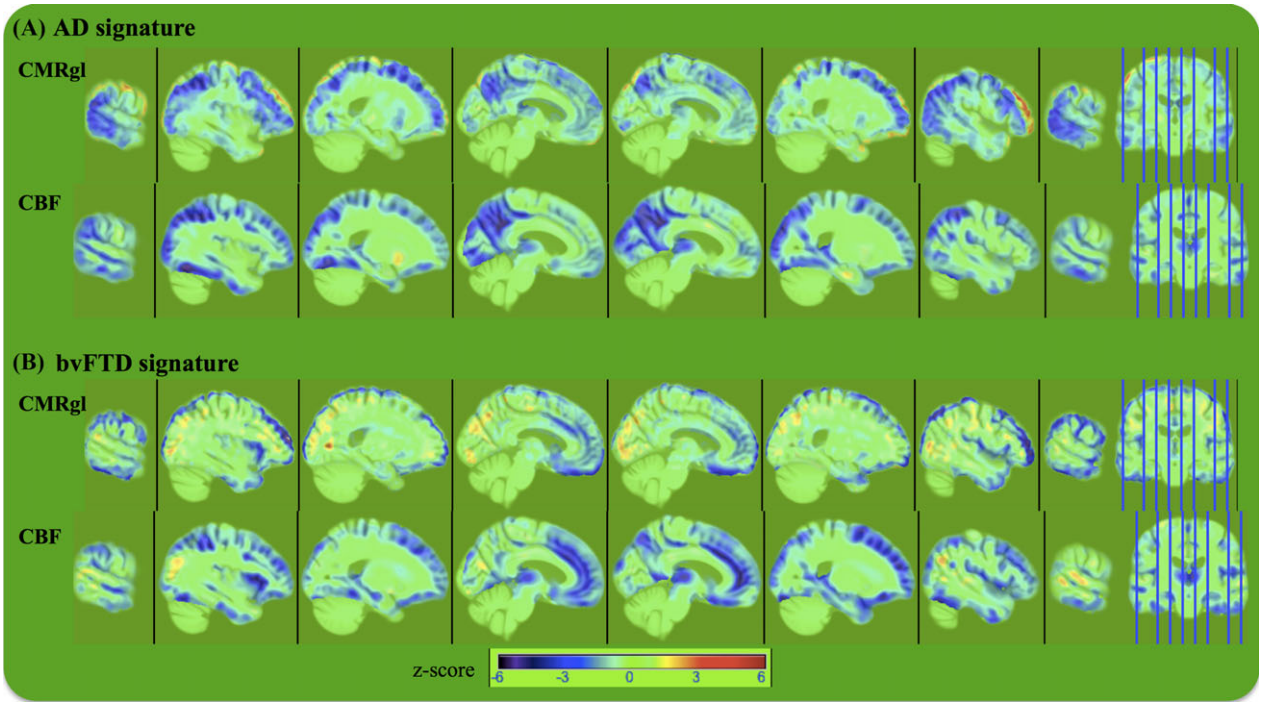

Figure 3. The spatial signature of the latent variables inferred by PLS logistic regression. Cold colors indicate hypoperfusion and hypometabolism detected by ASL-MRI and FDG-PET, respectively. Hot colors indicate hyperperfusion and hypermetabolism detected by ASL-MRI and FDG-PET, respectively. Dark red/blue colors indicate greater contribution of the local CMRgl and cerebral blood flow variations to the (A) AD versus CN and (B) bvFTD versus CN separation. Images are displayed in neurologic orientation. CN, cognitively normal controls; PLS, partial least squares.

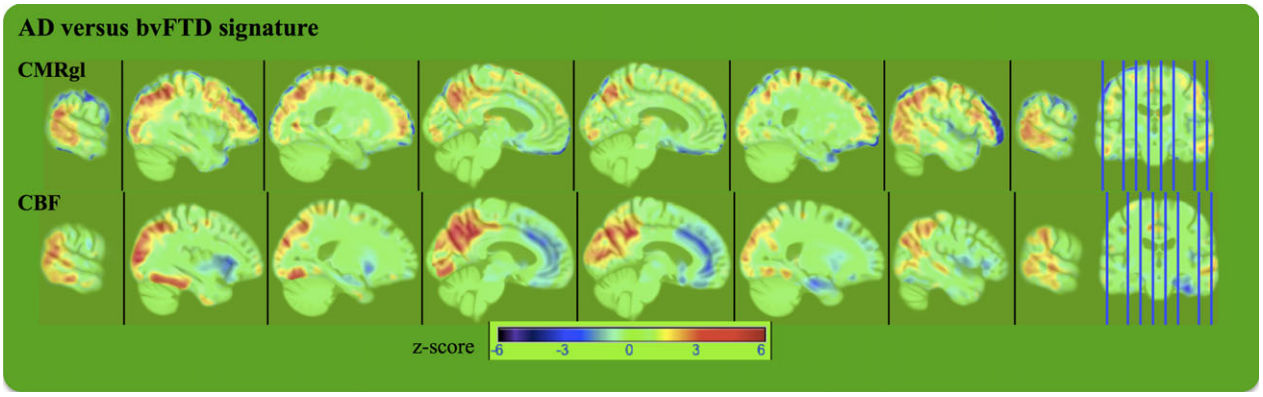

Figure 4. The spatial signature of the latent variables inferred by partial least squares logistic regression. Hot colors indicate hyperperfusion and hypermetabolism in bvFTD relative to AD detected by ASL-MRI and FDG-PET, respectively. Cold colors indicate hypoperfusion and hypometabolism in bvFTD relative to AD detected by ASL-MRI and FDG-PET, respectively. Dark red/blue colors indicate greater contribution of the local CMRgl and cerebral blood flow variations to the AD versus bvFTD separation. Images are displayed in neurologic orientation.

classification, with similar sensitivity (CMRgl-based 79%, CBF-based 78%) and specificity (CMRgl-based 100%, CBF-based 92%).

In differential classification of bvFTD and AD patients, area under the curve for CBF-based score (0.87, 95% CI: 0.75–0.99) was relatively greater than the AUC for CMRgl-based score (0.79, 95% CI: 0.57–1.00) without statistical significance ($P = 0.49$). Although both modalities performed similarly in terms of classifier sensitivity (CMRgl-based 89%, CBF-based 83%), CBF-based score had higher specificity than the CMRgl-based score (93% vs. 78%), again without statistical significance ($P = 0.10$).

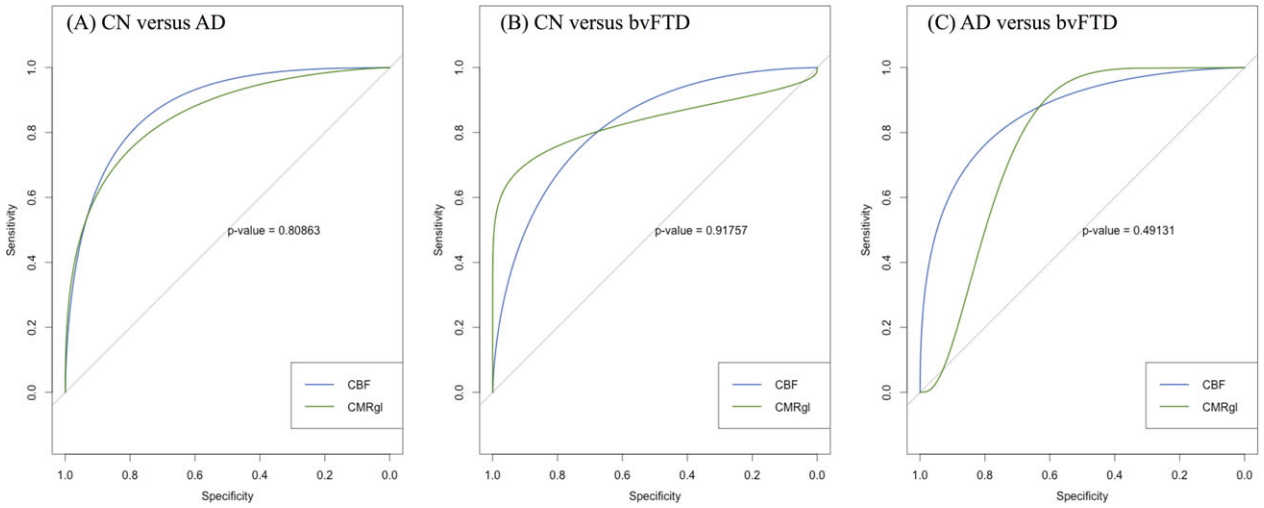

Figure 5. Receiver operating characteristic curves for discriminative power of CMRgl and cerebral blood flow changes in AD and bvFTD.

Table 2. Discriminative power of CBF and CMRgl changes in AD and bvFTD.

	AUC (95% CI)	Accuracy (95% CI)	Sensitivity (95% CI)	Specificity (95% CI)
CN versus AD				
CBF	0.89 (0.76–1.00)	88% (77–100)	86% (64–100)	92% (75–100)
CMRgl	0.91 (0.77–1.00)	90% (76–100)	78% (44–100)	100%
CN versus bvFTD				
CBF	0.83 (0.68–0.98)	83% (68–94)	78% (56–100)	92% (58–100)
CMRgl	0.85 (0.7–0.99)	87% (77–97)	79% (63–95)	100%
AD versus bvFTD				
CBF	0.87 (0.75–0.99)	86% (73–94)	83% (61–100)	93% (64–100)
CMRgl	0.79 (0.57–1.00)	86% (71–96)	89% (68–00)	78% (33–100)

AUC, areas under the curve; CBF, cerebral blood flow.

Discussion

The current study compared the diagnostic value of ASL-MRI with the value of FDG-PET in differentiating bvFTD, AD, and controls. The major finding is that the two imaging modalities showed comparable performance in differentiating each disorder from controls as well as from each other. While the maps of hypoperfusion look fairly similar to the maps of hypometabolism in both disorders relative to controls, spatial patterns of CBF and CMRgl changes that best separate the disorders differ especially in the temporal and medial frontal brain regions. We conclude that ASL-MRI, which can be obtained as part of an MRI examination, provides diagnostic information comparable to that obtained by FDG-PET.

This finding has implications for clinical care. Our cases were diagnosed after a multidisciplinary assessment at a subspecialty center. In the community, recognition of bvFTD is dependent on nonexpert clinicians, and diagnosis is often inaccurate.[5–7] Techniques that are less dependent on subjective interpretation provide an important adjunct to clinical assessment. This presumably motivated the decision by CMS to pay for FDG-PET for diagnosis of FTD, and the incorporation of imaging findings into the recently revised criteria for bvFTD.[31] Despite these recommendations, the optimal way to use imaging to support diagnosis remains uncertain. Brain imaging is usually interpreted in the community by visual inspection. Studies have indicated that community radiologists often fail to identify potentially diagnostic findings in structural MRIs.[48] While no studies have assessed the diagnostic accuracy of FDG-PET in FTD in community as opposed to academic settings, prior studies have demonstrated that visual interpretation of FDG-PET can accurately diagnose FTD,[49,50] and studies of AD have demonstrated that inter-reader agreement and confidence are higher for visual interpretation of FDG-PET compared with ASL-MRI.[26] This represents an advantage for FDG-PET, given current clinical practice. Ideally,

however, quantitative assessment could decrease the likelihood of missed findings for both ASL-MRI and FDG-PET. Further work with ASL-MRI to establish its suitability for visual interpretation and infrastructure improvements to promote more widespread quantification of brain imaging are both potential pathways to improve the utility of ASL-MRI as well as FDG-PET for diagnosis.

Our results are consistent with prior work, which showed that regional CBF is tightly coupled with regional cerebral metabolic rate for glucose,[51] and that patterns of regional perfusion abnormalities are very similar to the patterns of hypometabolism in AD.[27] In addition, prior studies have indicated that the diagnostic value of ASL-MRI is similar to that of FDG-PET in AD.[25,26] Several prior studies have shown that patterns of perfusion are different in AD and bvFTD,[18–20] and one prior study from Europe has supported the idea that diagnostic value of ASL-MRI is similar to the diagnostic value of FDG-PET.[19] The fact that two separate studies have now concluded that ASL-MRI has comparable diagnostic value to FDG-PET strengthens the argument that it should be a focus for continued development. The classification accuracies in our study are generally consistent with prior studies using FDG-PET, which have achieved accuracy rates of around 80–95%. However, it should be noted that most prior studies assessing classification accuracy in FTLD have used a mixed group of FTLD cases, including cases with the semantic and nonfluent variants of primary progressive aphasia (the exception is the European study referenced above[12,50]). Therefore, direct comparison of our classification outcomes with those of prior studies must be done with caution.

It is notable that the regions that contributed to classification in these two disorders were slightly different across modalities. Hypoperfusion was demonstrable in bvFTD compared with AD in several portions of the medial frontal lobes, insula, and amgydala, whereas predominantly lateral frontal brain regions were hypometabolic in bvFTD compared with AD. Furthermore, parietotemporal hypoperfusion in AD relative to bvFTD contributed to group separation, whereas a larger swath of hypometabolism in the medial occipitoparietal and frontal regions in AD relative to bvFTD contributed to group separation. These differences may relate to neurovascular decoupling, which has been identified as an early physiological abnormality in neurodegenerative disease.[52,53] On the other hand, differences in patterns of abnormalities might also be related to methodological differences in the way the ASL-MRI and FDG-PET data were processed and analyzed. CBF and CMRgl data are strongly affected by the underlying atrophy pattern.[54] We chose to assess noncorrected CBF and CMRgl quantitative maps because partial volume correction is not commonly used in clinical practice. However, the results from two modalities might be affected differently by the failure to account for partial volume effects coupled with differences in signal to noise ratio and spatial resolution. Furthermore, it is critically important to choose a reference region that robustly removes the unwanted variance in both CBF and CMRgl measures, but not the effects of the disease. The reference regions used in FDG-PET studies, such as pons and cerebellar vermis, are not easily used for ASL-MRI studies due to ASL-MRI's limited field of view and low signal to noise in inferior aspects of brain (i.e., arterial blood water is magnetically tagged below the brain). A reasonable approach when the question in the comparison is diagnostic utility is to use the optimal intensity normalization for each modality, as implemented in this study. Finally, the issue of whether ASL-MRI provides additional diagnostic value beyond structural MRI was not addressed in this article, and will be important to address in future work.

There were several limitations of the present study. Our conclusion that ASL and PET have similar diagnostic value rests on the fact that the errors in classification were relatively large, as expressed by the wide range in 95% CIs for AUC. The reliability of these classifications may improve with larger sample sizes, and this may reveal relative advantages for one technique or another. Our results may not precisely generalize to a general population since the predictive performance of the final classifier model was assessed using cross-validation. This, or related, approaches would need to be prospectively tested and refined for ease of use, especially for applicability in the clinical care setting. Second, both AD and bvFTD patients were identified by clinical diagnosis, but not autopsy confirmed. Therefore, to the extent that the diagnosis was inaccurate, the CBF and CMRgl features may reflect other pathologies than AD and bvFTD. On a similar note, we recognize that the inclusion of imaging in the current diagnostic criteria for bvFTD may have influenced the patterns of referrals to our study and caused us to overestimate the power of imaging for classification. Given that our primary goal was comparison of FDG-PET and ASL-MRI, this confound would not be very likely to affect our conclusion, which would be that ASL-MRI may have diagnostic value to the same extent as FDG-PET. In terms of the follow-up, we would point out a diagnosis of possible FTD does not preclude a diagnosis of dementia. For the most part, cases in whom we diagnose possible bvFTD have a dementia, but might not meet probable bvFTD because their images show atrophy, but not in a predominantly frontotemporal pattern. This has been well described, for instance, in patients with FTLD-causing mutations, in particular C9ORF72, who have atypical patterns of anatomical involvement and have in some cases

been labeled as having "FTD phenocopy."[55] We suspect that the imperfection in classification is in part due to the inclusion of these genetic cases, which would increase anatomical variability. This could be investigated as larger cohorts continue to accumulate. Furthermore, the bvFTD cohort included eight mutation carriers (PGRN, C9ORF72), and the patterns of CBF and CMRgl may differ between sporadic and genetic varieties of FTLD. Another limitation of this study is that we assessed the utility of ASL-MRI and FDG-PET in differential diagnosis of bvFTD and AD patients at the group level. These clinical cohorts are inherently heterogeneous in terms of underlying neurodegenerative patterns, therefore, potentially limiting the direct generalizability of our results to clinical diagnosis. A methodological limitation of this study is that our ASL measurements were conducted at a single TI, making the acquisition suboptimal for certain patient groups with greater effect potentially in patients with advanced disease pathophysiology. One approach could have been to perform multiple ASL measurements at various TIs to model arterial arrival time in addition to CBF. However, this approach would have required considerably long scan time, which is often impractical with demented patients as in this study.

Despite these limitations, the practical clinical implications of this report add to other reports[25–27] suggesting that ALS-MRI has a similar sensitivity and specificity to FDG-PET for detecting brain changes due to AD and bvFTD. MRI examinations are noninvasive without ionizing radiation. In contrast, FDG-PET scans require by an intravenous injection and exposure to ionizing radiation. The Center for Medicare Services (CMS) still allows Medicare payments for FDG-PET scans to distinguish AD from bvFTD. Based on our current results and previous reports in the literature, we conclude that ASL-MRI could ultimately replace FDG-PET for differentiation of bvFTD from AD.

Author Contributions

D. T. and H. J. R. conceptualized this study and developed the image processing and analysis frameworks, performed statistical tests, and wrote the manuscript. N. S. provided guidance in statistical analysis. G. D. R., N. A., and W. J. acquired and processed FDG-PET scans. M. W. W. and B. L. M. provided neurological interpretation, scientific advice, guidance, and helped improve the manuscript.

Acknowledgments

This work was supported by the National Institutes of Health Grant P01 AG019724-11, K24 AG045333, R01 AG032306, and P50 AG023501, The Hillblom Network, and the Department of Defense Grant W81XWH-05-2-0094. This work has also been made possible by use of research facilities at the Veteran Affairs Medical Center in San Francisco.

Conflicts of Interest

D. T., N. S., G. D. R., N. A., B. L. M., W. J., M. W. W., and H. J. R. report no conflicts of interest.

References

1. Ratnavalli E, Brayne C, Dawson K, Hodges JR. The prevalence of frontotemporal dementia. Neurology 2002;58:1615–1621.
2. Brunnstrom H, Gustafson L, Passant U, Englund E. Prevalence of dementia subtypes: A 30-year retrospective survey of neuropathological reports. Arch Gerontol Geriatr 2009;49:146–149.
3. Rosso SM, Donker Kaat L, Baks T, et al. Frontotemporal dementia in The Netherlands: patient characteristics and prevalence estimates from a population-based study. Brain 2003;126(Pt 9):2016–2022.
4. Kertesz A, Blair M, McMonagle P, Munoz DG. The diagnosis and course of frontotemporal dementia. Alzheimer Dis Assoc Disord 2007;21:155–163.
5. Woolley JD, Khan BK, Murthy NK, et al. The diagnostic challenge of psychiatric symptoms in neurodegenerative disease: rates of and risk factors for prior psychiatric diagnosis in patients with early neurodegenerative disease. J Clin Psychiatry 2011;72:126–133.
6. Varma AR, Snowden JS, Lloyd JJ, et al. Evaluation of the NINCDS-ADRDA criteria in the differentiation of Alzheimer's disease and frontotemporal dementia. J Neurol Neurosurg Psychiatry 1999;66:184–188.
7. Mendez MF, Shapira JS, McMurtray A, et al. Accuracy of the clinical evaluation for frontotemporal dementia. Arch Neurol 2007;64:830–835.
8. Foster NL, Heidebrink JL, Clark CM, et al. FDG-PET improves accuracy in distinguishing frontotemporal dementia and Alzheimer's disease. Brain 2007;130(Pt 10):2616–2635.
9. Raamana PR, Rosen H, Miller B, et al. Three-class differential diagnosis among alzheimer disease, frontotemporal dementia, and controls. Front Neurol 2014;5:71.
10. Ossenkoppele R, Prins ND, Pijnenburg YA, et al. Impact of molecular imaging on the diagnostic process in a memory clinic. Alzheimers Dement 2013;9:414–421.
11. Tripathi M, Tripathi M, Damle N, et al. Differential diagnosis of neurodegenerative dementias using metabolic phenotypes on F-18 FDG PET/CT. Neuroradiol J 2014;27:13–21.
12. Dukart J, Mueller K, Horstmann A, et al. Combined evaluation of FDG-PET and MRI improves detection and differentiation of dementia. PLoS ONE 2011;6:e18111.

13. Horn JF, Habert MO, Kas A, et al. Differential automatic diagnosis between Alzheimer's disease and frontotemporal dementia based on perfusion SPECT images. Artif Intell Med 2009;47:147–158.
14. Charpentier P, Lavenu I, Defebvre L, et al. Alzheimer's disease and frontotemporal dementia are differentiated by discriminant analysis applied to (99 m)Tc HmPAO SPECT data. J Neurol Neurosurg Psychiatry 2000;69:661–663.
15. Kobylecki C, Langheinrich T, Hinz R, et al. 18F-florbetapir PET in patients with frontotemporal dementia and Alzheimer disease. J Nucl Med 2015;56:386–391.
16. Bohnen NI, Djang DS, Herholz K, et al. Effectiveness and safety of 18F-FDG PET in the evaluation of dementia: a review of the recent literature. J Nucl Med 2012;53:59–71.
17. Jagust W, Reed B, Mungas D, et al. What does fluorodeoxyglucose PET imaging add to a clinical diagnosis of dementia? Neurology 2007;28:871–877.
18. Hu WT, Wang Z, Lee VM, et al. Distinct cerebral perfusion patterns in FTLD and AD. Neurology 2010;75:881–888.
19. Du AT, Jahng GH, Hayasaka S, et al. Hypoperfusion in frontotemporal dementia and Alzheimer disease by arterial spin labeling MRI. Neurology 2006;67:1215–1220.
20. Zhang Y, Schuff N, Ching C, et al. Joint assessment of structural, perfusion, and diffusion MRI in Alzheimer's disease and frontotemporal dementia. Int J Alzheimers Dis 2011;2011:546871.
21. McMurtray AM, Chen AK, Shapira JS, et al. Variations in regional SPECT hypoperfusion and clinical features in frontotemporal dementia. Neurology 2006;66:517–522.
22. Jeong Y, Cho SS, Park JM, et al. 18F-FDG PET findings in frontotemporal dementia: an SPM analysis of 29 patients. J Nucl Med 2005;46:233–239.
23. Ishii K, Sakamoto S, Sasaki M, et al. Cerebral glucose metabolism in patients with frontotemporal dementia. J Nucl Med 1998;39:1875–1878.
24. Grimmer T, Diehl J, Drzezga A, et al. Region-specific decline of cerebral glucose metabolism in patients with frontotemporal dementia: a prospective 18F-FDG-PET study. Dement Geriatr Cogn Disord 2004;18:32–36.
25. Verfaillie SC, Adriaanse SM, Binnewijzend MA, et al. Cerebral perfusion and glucose metabolism in Alzheimer's disease and frontotemporal dementia: two sides of the same coin? Eur Radiol 2015;25:3050–3059.
26. Musiek ES, Chen Y, Korczykowski M, et al. Direct comparison of fluorodeoxyglucose positron emission tomography and arterial spin labeling magnetic resonance imaging in Alzheimer's disease. Alzheimers Dement 2012;8:51–59.
27. Chen Y, Wolk DA, Reddin JS, et al. Voxel-level comparison of arterial spin-labeled perfusion MRI and FDG-PET in Alzheimer disease. Neurology 2011;77:1977–1985.
28. McKhann G, Drachman D, Folstein M, et al. Clinical diagnosis of Alzheimer's disease: report of the NINCDS-ADRDA Work Group under the auspices of Department of Health and Human Services Task Force on Alzheimer's Disease. Neurology 1984;34:939–944.
29. Neary D, Snowden JS, Gustafson L, et al. Frontotemporal lobar degeneration: a consensus on clinical diagnostic criteria. Neurology 1998;1998:1546–1554.
30. Kramer JHP, Jurik JMA, Sha SJMS, et al. Distinctive neuropsychological patterns in frontotemporal dementia, semantic dementia, and Alzheimer disease. Cogn Behav Neurol 2003;16:211–218.
31. Rascovsky K, Hodges JR, Knopman D, et al. Sensitivity of revised diagnostic criteria for the behavioural variant of frontotemporal dementia. Brain 2011;134(Pt 9):2456–2477.
32. Folstein MF, Folstein SE, McHugh PR. "Mini-mental state". A practical method for grading the cognitive state of patients for the clinician. J Psychiatr Res 1975;12:189–198.
33. Kaplan E, Goodglass H, Weintraub S. The Boston Naming Test, 2nd ed. Philadelphia: Lea & Febiger, 1983.
34. Reitan R. Validity of the trail making test as an indicator of organic brain damage. Percept Mot Skills 1958;8:271–279.
35. Delis DC, Kaplan E, Kramer JH. Delis-Kaplan Executive Function System. San Antonion, TX: The Psychological Corporation, 2001.
36. Yesavage JA, Brink TL, Rose TL, et al. Development and validation of a geriatric depression screening scale: a preliminary report. J Psychiatr Res 1982;17:37–49.
37. Morris JC. The clinical dementia rating (CDR): current version and scoring rules. Neurology 1993;43:2412–2414.
38. Wolf RL, Detre JA. Clinical neuroimaging using arterial spin-labeled perfusion magnetic resonance imaging. Neurotherapeutics 2007;4:346–359.
39. Furst AJ, Rabinovici GD, Rostomian AH, et al. Cognition, glucose metabolism and amyloid burden in Alzheimer's disease. Neurobiol Aging 2012;33:215–225.
40. Tosun D, Mojabi P, Weiner MW, Schuff N. Joint analysis of structural and perfusion MRI for cognitive assessment and classification of Alzheimer's disease and normal aging. NeuroImage 2010;52:186–197.
41. Lehmann M, Ghosh PM, Madison C, et al. Diverging patterns of amyloid deposition and hypometabolism in clinical variants of probable Alzheimer's disease. Brain 2013;136(Pt 3):844–858.
42. Minoshima S, Frey KA, Foster NL, Kuhl DE. Preserved pontine glucose metabolism in Alzheimer disease: a reference region for functional brain image (PET) analysis. J Comput Assist Tomogr 1995;19:541–547.
43. Greve DN, Fischl B. Accurate and robust brain image alignment using boundary-based registration. NeuroImage 2009;48:63–72.
44. Avants BB, Tustison NJ, Song G, et al. A reproducible evaluation of ANTs similarity metric performance in brain image registration. NeuroImage 2011;54:2033–2044.

45. Wold S, Geladi P, Esbensen K, Öhman J. Multi-way principal components-and PLS-analysis. J Chemom 1987;1:41–56.
46. Jolliffe IT. A note on the use of principal components in regression. J R Stat Soc Ser C Appl Stat 1982;31:300–303.
47. Mc NQ. Note on the sampling error of the difference between correlated proportions or percentages. Psychometrika 1947;12:153–157.
48. Suarez J, Tartaglia MC, Vitali P, et al. Characterizing radiology reports in patients with frontotemporal dementia. Neurology 2009;73:1073–1074.
49. Foster NL, Heidebrink JL, Clark CM, et al. FDG-PET improves accuracy in distinguishing frontotemporal dementia and Alzheimer's disease. Brain 2007;130:2616–2635.
50. Rabinovici GD, Rosen HJ, Alkalay A, et al. Amyloid vs FDG-PET in the differential diagnosis of AD and FTLD. Neurology 2011;77:2034–2042.
51. Jueptner M, Weiller C. Review: does measurement of regional cerebral blood flow reflect synaptic activity? Implications for PET and fMRI NeuroImage 1995;2:148–156.
52. Ruitenberg A, den Heijer T, Bakker SL, et al. Cerebral hypoperfusion and clinical onset of dementia: the rotterdam study. Ann Neurol 2005;57:789–794.
53. Knopman DS, Roberts R. Vascular risk factors: imaging and neuropathologic correlates. J Alzheimers Dis 2010;20:699–709.
54. Muller-Gartner HW, Links JM, Prince JL, et al. Measurement of radiotracer concentration in brain gray matter using positron emission tomography: MRI-based correction for partial volume effects. J Cereb Blood Flow Metab 1992;12:571–583.
55. Sha SJ, Takada LT, Rankin KP, et al. Frontotemporal dementia due to C9ORF72 mutations: clinical and imaging features. Neurology 2012;79:1002–1011.

